Cellulose (2024) 31:5707–5723
https://doi.org/10.1007/s10570-024-05844-6

ORIGINAL RESEARCH

Passive daytime radiative cooling aerogels based on wollastonite particle-embedded cellulose for energy-saving buildings

Chen Deng · Bencheng Zhao · Zhuoqun Wang · Xuejie Yue · Dongya Yang · Fengxian Qiu

Received: 10 August 2023 / Accepted: 5 March 2024 / Published online: 10 May 2024

Abstract Passive daytime radiative cooling (PRDC) is a promising technology providing a cooling strategy that radiates heat directly into outer space without additional energy consumption, a crucial consideration in controlling construction energy consumption. However, the preparation of PRDC materials with controlled radiative properties is still challenging because the radiative interface must be maintained in a clean environment. Herein, a densely distributed porous hybrid aerogel with controlled radiative properties was fabricated using the wollastonite and cellulose as building blocks for building energy-saving applications. To do this, the cellulose pulp was obtained by using waste paper as raw material. Then, the hybrid aerogels, comprising paper cellulose and wollastonite particles, were fabricated by combining the acrylic acid polymers (PAA) bonding, freeze drying and vapor deposition modification. The radiative cooling hybrid aerogel exhibits high solar reflectivity (94.6%) and high atmospheric emissivity (95.1%), due to the laminated design of wollastonite randomly dispersed in the radiative hybrid aerogel. The excellent PRDC capability is also proven by outdoor tests where practical temperature difference is ~ 6.3 ℃ and the maximum cooling power of 147.4 Wm^{-2} under direct sun irradiance. Wettability test infers that the hybrid aerogel has a static water contact angle of 144.07° ± 2°, thereby indicating its hydrophobicity. In addition, based on the Energyplus simulation, the hybrid aerogel exhibits an average annual cooling energy saving of 8% in buildings across China. The excellent radiative cooling and self-cleaning properties of hybrid aerogel make it durable for long-term outdoor PRDC applications.

Keywords Wollastonite · Passive radiative daytime cooling · Cellulose · Building energy efficiency · Self-cleaning

Supplementary Information The online version contains supplementary material available at https://doi.org/10.1007/s10570-024-05844-6.

C. Deng · B. Zhao · X. Yue · D. Yang (✉) · F. Qiu
Institute of Green Chemistry and Chemical Technology, Jiangsu University, Zhenjiang 212013, Jiangsu Province, China
e-mail: yangdyxxb@ujs.edu.cn

Z. Wang
Department of Mechanical and Electrical Engineering, Hebei Vocational University of Technology and Engineering, Xingtai, China

Introduction

The building industry currently accounts for approximately 46% of total national energy consumption. Around half of the energy is consumed in buildings operations, which includes the illumination, heating, and cooling ventilation systems (Chai and Fan 2022). Over the last decade, the provision of building cooling has remained a crucial element in ensuring thermal comfort across various commercial and residential settings (She et al. 2018). Traditional electrical cooling equipment is based on the vapor compression cycle, which requires high energy consumption, as well as refrigerant gases with possible health hazards. Meanwhile, due to this cooling process involving converting work into heat, traditional cooling strategy simply transfers heat from one part of the Earth's surface to another causing net heating effect. The high-energy consumption and refrigerant of cooling equipment have raised widespread concerns about environmental problems, such as global warming (He et al. 2023), ozone depletion (Xue et al. 2023) and indoor air quality (Cheng et al. 2019). Therefore, in recent years, considerable attention has been focused on the design of building energy-saving materials to achieve thermal comfort. One of the most effective strategies for building energy conservation is to design of photovoltaic buildings via regulation of chemical compositions and microstructures of photovoltaic materials. However, photovoltaic buildings have some disadvantages owing to technical constraints and economic obstacles, such as low energy-conversion, high cost and poor adaptability to climate and environmental fluctuations. Therefore, the development of functional materials with low cost and stable properties revels great significance in building energy-saving.

Passive radiative cooling is a novel cooling method in which one hot object radiates heat into outer space through the atmospheric transparency window (8 – 13 μm) in the form of blackbody radiation, which has great potential for cooling buildings (Yue et al. 2022; Zhao et al. 2022b), vehicles (Soulios et al. 2018), and solar cells (Zhao et al. 2022a). Passive radiative cooling technology provides an alternative to traditional air conditioning refrigeration on buildings to reduce electrical costs because it uses no energy. For example, Lin et al. (2021) proposed a PDMS-silica-silver radiative cooler, which resulted in a sub-ambient temperature drop of ~ 4.8 ℃. Compared to a standard air conditioning system, the cooler could achieve energy savings of around 17%. A high mid-IR emission allows materials to effectively dissipate heat into cold universe. As a consequence, materials can be easily cooled below sub-ambient, especially at night (Jing et al. 2021). In this regard, Meir et al. (2002) reported a radiative cooling system consisting of modified PPO as a radiator, water as a heat carrier, and the system could achieve 20 ℃ lower than environment temperature at night. Meanwhile, Chen et al. (2020) designed PET aluminized coatings with weather resistance and anti-ultraviolet capability, which exhibited a nighttime temperature drop of up to 4 ℃. However, it is challenging to achieve sub-ambient cooling during the day since the absorption of intense sunlight easily exceeds the heat dissipation by thermal emission. As a result, to achieve building energy savings, passive daytime radiative cooling (PRDC) is still required for practical applications, as most end-users use their equipment during the daytime, which leads to high-energy consumption. To realize passive daytime radiative cooling (PRDC), a material must with both high solar reflectance (0.25–2.5 μm) and strong mid-infrared (MIR) emissivity.

Inorganic materials containing elements such as aluminum, silicon, calcium, and titanium exhibit high emissivity in the atmospheric window and high reflectivity in the visible region and are frequently used in architectural coatings (Song et al. 2014). For example, Rephaeli et al. (2013) designed a metal-dielectric photonic structure for PRDC structure to achieve daytime radiative cooling and selective emission in the atmospheric transparency window by utilizing the excellent optical properties of silicon dioxide (SiO_2) and hafnium dioxide (HfO_2). Subsequently, Lin et al. (2022) fabricated a dual-layer structure of TiO_2-PDMS/Al_2O_3-PDMS with a solar spectrum reflectivity of 92.2% and an infrared emissivity of 95.3%. This material achieved a 1.5 ℃ sub-ambient cooling effect and an average radiative cooling power of 79 Wm^{-2}. However, the large-scale application of these advanced cooling materials is still limited because of the multiple processes required to obtain them. Wollastonite as an emerging mineral raw material, which has excellent thermal and chemical stability, but it is rare to use wollastonite as radiative cooling material (Kangal et al. 2020). At the same time, wollastonite has the characteristics of high infrared emission and high sunlight reflection, so it is a kind of potential cooling material. In another work, Zhang et al. (2022) prepared composite cellulose acetate film with containing randomly distributed wollastonite particles by phase transformation method. The film achieves a cooling of 7.3 ℃ in direct sunlight and an average net cooling power of 90.7 Wm^{-2}. Although the wollastonite has been successfully applied in buildings, it still has some disadvantages, including poor dispersibility, low stability, complex preparation and large energy consumption. Therefore, the application of wollastonite in radiative cooling materials will face a series of problems (e.g. wollastonite size, selection of supporting substrate and cross-linking agent and preparation process), which is still a major challenge for the large-scale application of wollastonite.

Herein, the present study provides a simple and replicable preparation method for wollastonite/cellulose hybrid aerogel for building energy-saving applications. The Trimethoxymethylsilane (MTMS)-modified hybrid aerogel with stabilized radiative cooling properties was obtained through acrylic acid polymers (PAA) bonding, and vacuum freeze-drying, followed by hydrophilization with chemical vapor deposition. Due to the random dispersion of wollastonite in the aerogel, even without metal back-coating, the MTMS-modified hybrid aerogel exhibits high solar reflectivity (94.6%) and an extremely high atmospheric window emissivity (95.1%) simultaneously. The radiative cooling test showed that the MTMS-modified hybrid aerogel could be cooled 6.3 ℃ lower than the ambience under direct solar irradiance (400 W m^{-2}), which is 2 ℃ cooler than the cellulose aerogel. Theoretical results show that the average radiative cooling power for MTMS-modified hybrid aerogel was 147.4 W m^{-2} with the daytime irradiance of 1000 W m^{-2}. Thermal stability test suggests that the pyrolysis temperature of the hybrid aerogel is 230 ℃, indicating it has strong thermal stability and can adapt to the harsh high-temperature environment. Meanwhile, the MTMS-modified hybrid aerogel possessed great hydrophobicity with static water contact angle of $144.07° \pm 2°$, indicating that the aerogel has outstanding self-cleaning performance. Consequently, the MTMS-modified hybrid aerogel not only increases the sunlight reflection as well as the thermal emission from the material, but also solves the problems of wollastonite in radiative materials such as poor dispersion and uneven particle size, while maintaining the self-cleaning property, which is favorable for long-term outdoor applications.

Experimental section

Materials

Waste paper handkerchief were collected from the campus of Jiangsu University (Zhenjiang, China). Wollastonite and Acrylic acid Polymers (PPA) were obtained by Sopo (Zhenjiang) Co. Ltd. Trimethoxymethylsilane (MTMS, $\geq 99.8\%$), Tert-butylalcohol (TBA, $\geq 99.5\%$), Ethanol absolute (C_2H_8O, $\geq 99.5\%$) and Hydrochloric acid (HCl, 36%) were purchased from Sinopharm Chemical Reagents Co. Ltd (Shanghai, China). Deionized water was obtained the laboratory water-purifying system (Zhenjiang, China). All chemicals were analytically pure without further purification, and distilled water was used throughout the process.

Preparation of the wollastonite/cellulose hybrid aerogel

The wollastonite/cellulose hybrid aerogel was prepared by a simple freeze-drying method using waste paper handkerchief and wollastonite nanoparticles as raw materials. In a typical preparation procedure, the waste handkerchief (about 1 g) was cut into small stands (1 cm × 3 cm) and stirred in 500 mL of DI water and 2 mL of 12 mol/L of HCl for 12 h to form cellulose pulp. The cellulose pulp was washed by vacuum filtration cleaning using deionized water and ethyl alcohol to neutral and dried in an oven at 80 ℃. Then, 1 g of dried cellulose and 3 g of wollastonite were added into beaker with 22.5 mL of 24.7 mol/L tert-butylalcohol solution under continuous stirring for 10 min at a temperature of 30 °C to form the composite cellulose solution. Afterwards, 1 mL of PPA was dispersed into deionized water (3 mL) under ultrasonication for 15 min. The cellulose composite solution was mixed with PPA content (25 wt%) under magnetic stirring for 30 min followed by 15 min of ultrasonication to a suspension. Finally, the suspension was poured into a cylindrical mold (φ = 8 cm) and frozen at -15 ℃ for 12 h before subsequent drying under vacuum at -60 ℃ for 48 h to form the wollastonite/cellulose hybrid aerogel.

Surface modifying of wollastonite/cellulose hybrid aerogel

To maintain stable radiative cooling wollastonite/cellulose hybrid aerogel, the surfaces of wollastonite/cellulose hybrid aerogel were modified with by hydrophobic via the chemical vapor deposition (CVD) method (Zhu et al. 2023). Typically, the obtained wollastonite/cellulose hybrid aerogel was placed in the glass chamber with two polytetrafluoroethylene vials of MTMS (1 mL) and DI water (1 mL) and then heated at 70 ℃ for 8 h to undergo silanization process. After that, the wollastonite/cellulose hybrid aerogel was placed in a vacuum oven at 60 ℃ for 6 h to remove superfluous MTMS. The preparation process of the MTMS-modified wollastonite/cellulose hybrid aerogel is illustrated in Fig. 1.

Characterization

The microstructures and morphologies of the resultant samples were studied by a field-emission scanning electron microscope (SEM, JEOL JSM-7800F, Japan) and elemental mapping (EDS), which was operated at 10 kV. Before observation, the aerogels were attached to the SEM samples stage with a carbon conductive adhesive and then sputter-coated with a gold–palladium. The X-ray diffraction patterns of the resultant aerogels in the diffraction angle (2θ) range from 10° to 80° at a scanning speed of 2° min^{-1} were conducted on an X-ray diffractometer (XRD, Bruker, Germany) equipped with Cu-Kα adiation (($\lambda = 0.15444$ nm) at an anode voltage of 40 kV and a current of 30 mA. The thermal stability of the MTMS-modified wollastonite/cellulose hybrid aerogel and the MTMS-modified cellulose aerogel were characterized by a nitrogen atmosphere using thermogravimetric analyzer (TGA). The thermal conductivity of aerogels was tested by a hot disk transient plane source (TPS) method through a thermal constant analyzer (Hot Disk TPS 2500S). The surface elements of the as-prepared materials were studied the X-ray surface photoelectron spectroscopy (XPS, Thermo Scientific K-Alpha, America). The samples were analyzed by FT-IR in attenuated total reflectance (ATR) mode using a Thermo Nicolet spectrometer equipment. Three parallel experiments were conducted for each analysis.

Solar reflectance and spectral emissivity calculation

The spectral solar reflectance from 0.25–2.5 μm of sample was recorded on a UV–vis-near-infrared (NIR) spectrophotometer with $BaSO_4$ white reference plate. the averaged solar reflectance R_{solar} was obtained in accordance with equation (Cai et al. 2023b; Xiang et al. 2021)

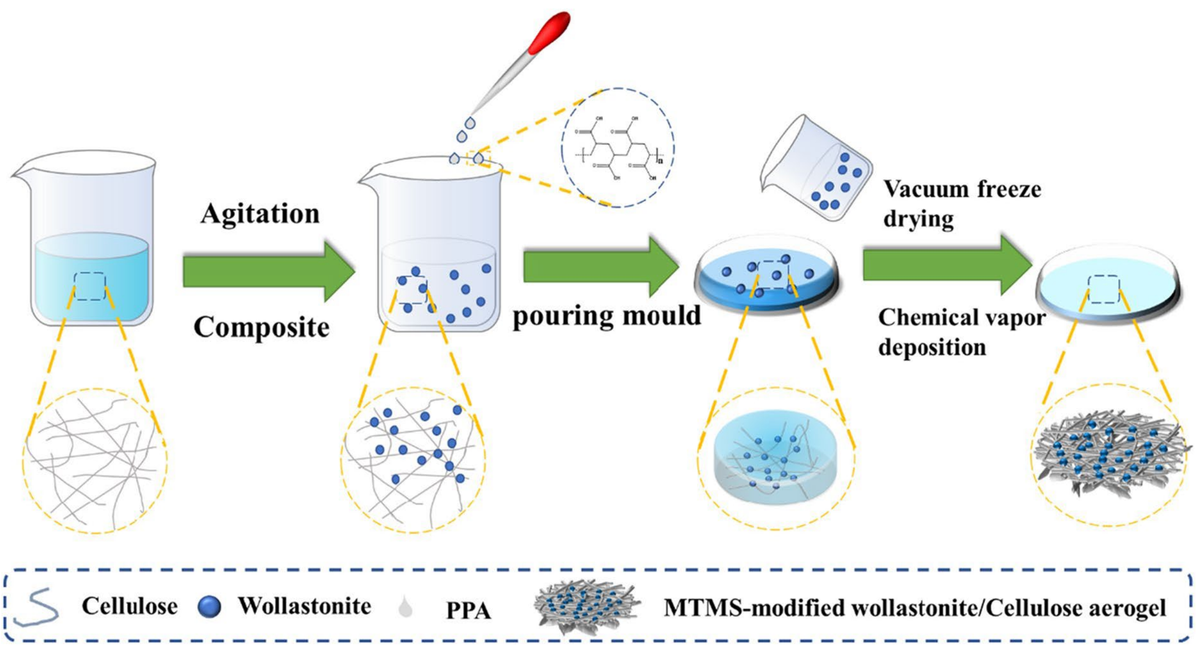

Fig. 1 Schematic illustration for the fabrication of the MTMS-modified wollastonite/cellulose hybrid aerogel

$$\overline{R}_{solar} = \frac{\int_{0.25\mu m}^{2.5\mu m} I_{solar}(\lambda)R(\lambda)d\lambda}{\int_{0.25\mu m}^{2.5\mu m} I_{solar}(\lambda)d\lambda} \quad (1)$$

where, R(λ) is the reflectance of the samples at wavelength λ, $I_{solar}(\lambda)$ represented the solar power (AM 1.5G).

The reflectance (R) and transmittance (T) spectrum within from 2.5 to 25 μm wavelength were characterized by using an FI-IR spectrometer equipped with a gold-coated integrating sphere at room temperature. According to Kirchhoff's, the emittance (ε) (2.5–25 μm) equal to absorption is calculated according to the equation: $\varepsilon = 1-$ T-R. The average value of infrared emissivity was defined as (Cai et al. 2023a; Li et al. 2023).

$$\overline{\varepsilon}_{LWIR} = \frac{\int_{8\mu m}^{13\mu m} I_{LWIR}(\lambda)\varepsilon(\lambda)d\lambda}{\int_{8\mu m}^{13\mu m} I_{LWIR}(\lambda)d\lambda} \quad (2)$$

where, ε(λ) is the emittance of the sample at wavelength λ, and $I_{LWIR}(\lambda)$ represented the atmospheric transmission. Three parallel tests were conducted for each sample, and the average of three measurements was taken as the final result.

Radiative cooling properties

All experiments to investigate radiative cooling performance of cellulose aerogel were conducted in Zhen jiang, Jiangsu University. The device is mainly composed of the box made of polystyrene (PS) foam with a size of 45 cm × 25 cm × 20 cm. At the same time, three cavities of 6 cm × 6 cm × 1 cm were prepared at the top of the foam, and the PS foam with cavities was placed in the box, and the surface of two cavities was covered with different sample, and then place the foam box at a height of 50 cm from the ground to decrease thermal convection and thermal conduction between the resultant samples and the ground. The foam box was wrapped with aluminum foil to reflect sunlight, and the top was covered with a low-density polyethylene (PE) film. Two thermocouples are inserted in different cavities to record the cooling temperature, the extra thermocouple was placed in the cavity under the PE film of the uncovered sample to measure the ambient temperature.

Self-cleaning properties

To evaluate the self-cleaning properties of the MTMS-modified wollastonite/cellulose hybrid aerogel, the hydrophobicity of the composite aerogel before and after modification was measured by static contact angle (CA) measuring instrument. A drop of 5 μL deionized water droplet was placed horizontally on the sample table, and the contact angle of the droplet on the sample surface was recorded and measured by a contact angle measuring instrument in the ground gravity field environment. The test was performed at different positions on the surface of the MTMS-modified wollastonite/cellulose hybrid aerogel, and the average of three measurements was taken as the final result.

Result and discussion

To investigate the morphology evolution during the surface modification, the SEM images of MTMS-modified cellulose aerogel and MTMS-modified wollastonite/cellulose hybrid aerogel are shown in Fig. 2. The average thickness of MTMS-modified cellulose aerogel and MTMS-modified wollastonite/cellulose hybrid aerogel was found to be 1 cm. The porous morphology can be maintained by the application of the freeze-drying technique as shown in Fig. 2a. Therefore, the MTMS-modified cellulose has three-dimensional network morphology with porous structure (Fig. 2b), which is a critical factor for formation of hydrophobic interfaces and stable radiative properties of cellulose aerogel. A magnified SEM image shown in Fig. 2c reveals that the aerogel consists of cellulose fibers with irregular morphology. In addition, it can be seen that the MTMS-modified hybrid still retains the inherent three-dimensional porous network structure, indicating that the cross linking of PPA not affect the formation of the structure. It is indicated in Fig. 2d that the hybrid aerogels are comprised of winding cellulose fibers and wollastonite particles. Notably, the wollastonite possesses a long needle-like structure and firmly adheres to the surface of the fibers. The roughness and stability could be further enhanced via the addition of wollastonite and MTMS chemical vapor deposition reaction, respectively. Meanwhile, in previous studies (Mandal

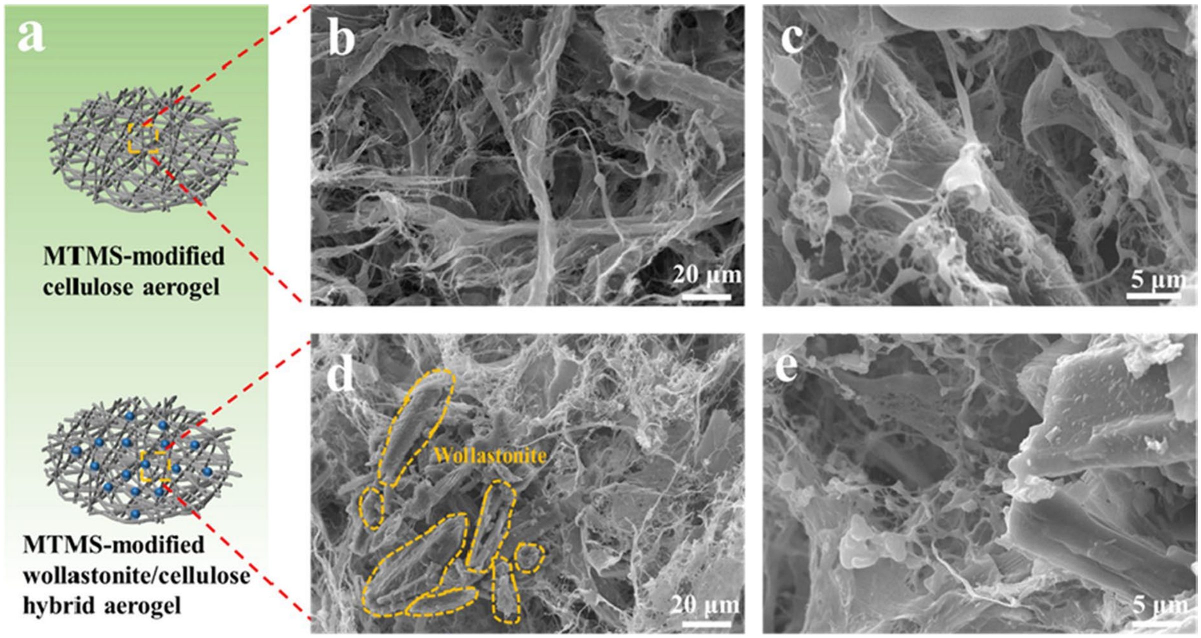

Fig. 2 Schematic illustration of structural features of MTMS-modified cellulose aerogel and MTMS-modified wollastonite/cellulose hybrid aerogel (**a**), SEM images of MTMS-modified cellulose aerogel (**b** and **c**) and MTMS-modified wollastonite/cellulose hybrid aerogel (**d** and **e**)

et al. 2018), the broadly distributed pores can effectively achieve Mie scattering. As shown in Fig. 2e, a large number of fibers and wollastonite formed porous structures, which proved to be consistent with the scattering theory to enhance the reflectance of sunlight. The energy-dispersive spectral (EDS) mapping shown in Fig. S1(Supporting Information), demonstrated that the wollastonite was irregularly distributed in the cellulose matrix, and hydrophobic surfaces could be clearly observed from the silicon element. In other words, freeze-drying technology was used to successfully cross-link wollastonite and cellulose by PPA to form hybrid aerogel with porous structure, while the success of hydrophobic modification by deposition of MTMS was demonstrated.

To investigate the structural transformation during surface grafting, the crystal phase and purity of the samples were characterized by XRD, and the XRD characterization results are shown in Fig. 3 and Fig. S2. The MTMS-modified cellulose aerogel exhibited the diffraction peaks at $2\theta = 14.7°$, 16.5° and 22.6°, assigned to the $(1\ \bar{1}\ 0)$, (1 1 0) and (2 0 0) planes of cellulose Iβ (Fig. 3a), respectively (Li et al. 2021). As shown in Fig. S2, there were no obvious change in the crystal structure of cellulose aerogel after surface modification, meaning the crystal phase of cellulose aerogel was unchanged. Wollastonite exhibits typical mineral structure planes at $2\theta = 11.8°$,

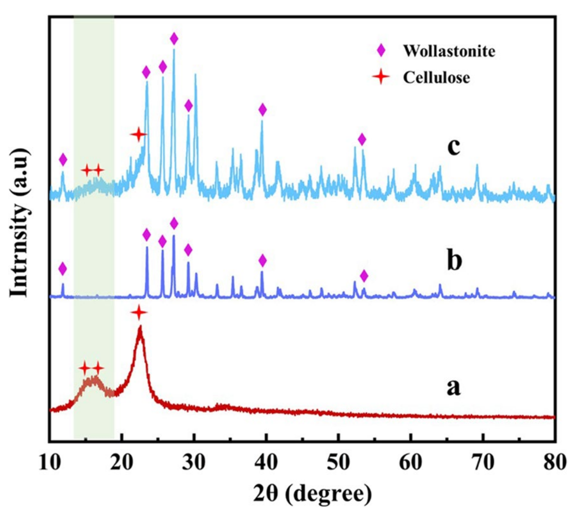

Fig. 3 XRD patterns of the different kinds of samples: MTMS-modified cellulose aerogel (**a**), wollastonite (**b**), MTMS-modified wollastonite/cellulose aerogel (**c**)

23.5°, 25.5°, 27.1°, 29.2°, 39.4° and 53.5° (Fig. 3b), which are attributed to the basal reflections of (2 0 0), (-3 1 1), (0 0 2), (-2 0 2), (-2 1 2), (-2 0 3) and (-7 2 2), respectively (Zheng et al. 2021). The diffraction peaks for the MTMS-modified wollastonite/cellulose hybrid aerogel at 14.7°, 16.5°, and 22.6° were not obvious (Fig. 3c), this was probably due to that the characteristic peaks of cellulose were partially obscured. When wollastonite was introduced into the cellulose aerogel system does not destroy the crystal due to the successful physical cross-linking process between wollastonite and cellulose, benefiting from plenty of -OH groups of wollastonite (Shang et al. 2021) (Fig. S3). Meanwhile, the crystal structure of wollastonite in the hybrid cellulose aerogel remained unchanged before and after hydrophobic modification, indicating that the crystalline structures of wollastonite was not affected by surface grafting of MTMS.

To explore the reaction mechanism of cellulose aerogel by MTMS modification, the functional groups of samples were analyzed by FT-IR spectra. FT-IR spectra of cellulose aerogel, wollastonite/cellulose hybrid aerogel and MTMS-modified wollastonite/cellulose hybrid aerogel are shown in Fig. 4A. All peaks appearing at 2957 cm^{-1} were attributed to the C-H stretching vibration in the cellulose aerogel (Fig. 4A(a)), with the peaks at and 1030 cm^{-1} assigned to the C–O–C stretching vibration (Li et al. 2019). The wollastonite/cellulose hybrid aerogel (Fig. 4A(b)) and MTMS-modified wollastonite/cellulose hybrid aerogel (Fig. 4A(c)) showed two emerging characteristic peaks at 511 cm^{-1} and 644 cm^{-1}, which were attributed to the stretching vibration of Ca-O and stretching vibration of Si–O-Si (Sun et al. 2013), respectively. The stretching vibration peak of C=O of the crosslinking agent PPA appears at 1724 cm^{-1}, indicating that the wollastonite was successfully linked with cellulose via PPA. The MTMS-modified wollastonite/cellulose hybrid aerogel appearing new characteristic bands at 781 cm^{-1} and 1274 cm^{-1} were usually detected inside of the hydrophobic group, and they represent the stretching and bending vibration of Si-CH_3, indicating that the -CH_3 have been grafted on the surfaces of wollastonite/cellulose hybrid aerogel. In addition, the broad peak centered at 3340 cm^{-1} assigned to the stretching vibration of the hydroxyl groups (Wang and Liu 2019). The intensity of the hydroxyl groups in MTMS-modified wollastonite/cellulose hybrid aerogel clearly decreased compared with the wollastonite/cellulose hybrid aerogel, which indicated that the condensation reaction was taken place between the hydroxyl groups in the wollastonite/cellulose hybrid aerogel and MTMS. The probable reaction mechanism for MTMS modification of wollastonite/cellulose hybrid aerogel is shown in Fig. 4B. When wollastonite/cellulose hybrid aerogel was treated with MTMS, MTMS was first hydrolyzed

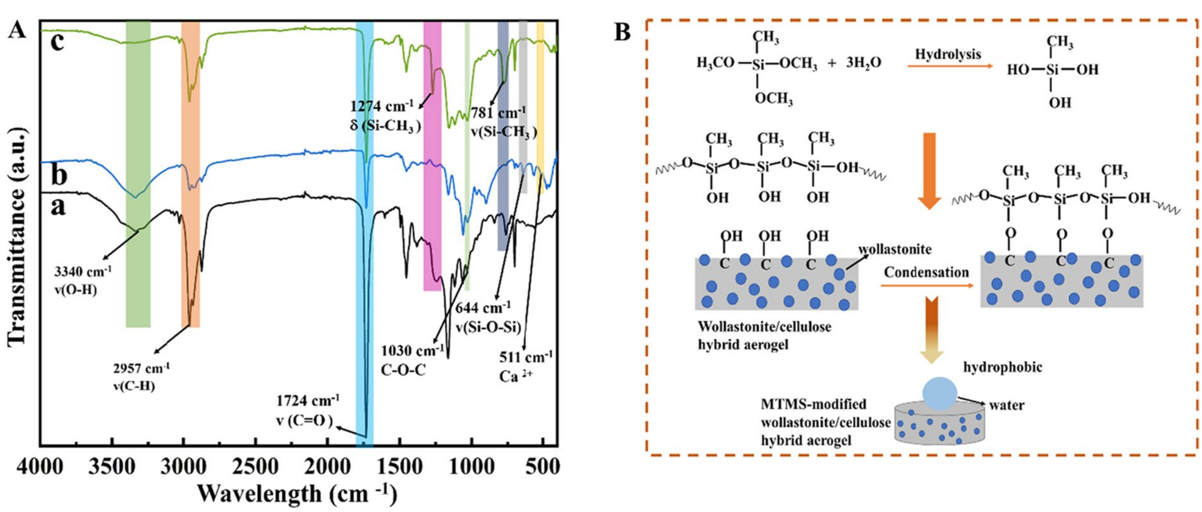

Fig. 4 **A** FT-IR spectra of cellulose aerogel (**a**), wollastonite/cellulose hybrid aerogel (**b**), MTMS-modified wollastonite/cellulose hybrid aerogel (**c**). **B** Possible reaction mechanism of MTMS with wollastonite/cellulose hybrid aerogel

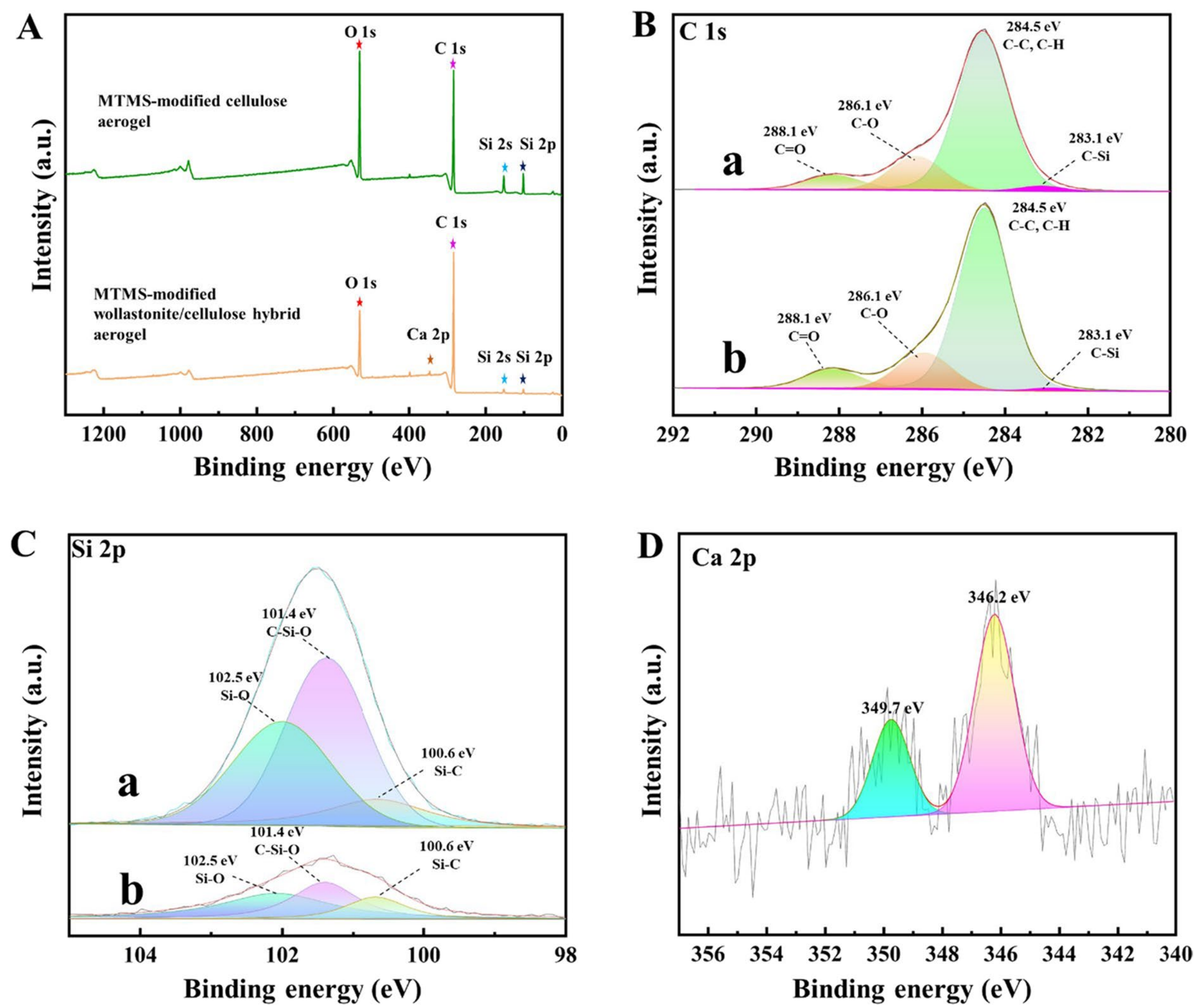

Fig. 5 **A** XPS survey spectra of MTMS-modified cellulose aerogel and MTMS-modified wollastonite/cellulose hybrid aerogel. High-resolution C 1 s (**B**)and Si 2p (**C**)spectra: MTMS-modified cellulose aerogel (**a**), MTMS-modified wollastonite/cellulose hybrid aerogel (**b**). **D** High-resolution Ca 2p spectra of MTMS-modified wollastonite/cellulose hybrid aerogel

to trisilanol, which was further condensed to oligonmers. Subsequently, the free -OH groups in trisilanol and oligomers and oligomers with -OH groups in wollastonite/cellulose hybrid aerogel were co-condensed. After curing, the resulting polymethysiloxane was covalently grafted onto wollastonite/cellulose hybrid aerogel. Therefore, the covalent grafting of $-CH_3$ groups is responsible for the hydrophobic property of the MTMS-modified wollastonite/cellulose hybrid aerogel.

XPS was performed to investigate the effective crosslinking between cellulose and wollastonite and the successful grafting reaction of $-CH_3$ groups onto the wollastonite/cellulose hybrid aerogel, and the XPS results of MTMS-modified cellulose aerogel and MTMS-modified wollastonite/cellulose hybrid aerogel were illustrated in Fig. 5. As expected, in addition to C 1 s and O 1 s signals associated with cellulose, there were two new peaks at about 153.0 eV and 102.5 eV for MTMS-modified cellulose aerogel, which was ascribed to Si 2 s and Si 2p, respectively (Tang et al. 2023). As shown in Fig. 5A, compared with MTMS-modified cellulose aerogel, the Ca 2p peak appears in the XPS spectrum of MTMS-modified wollastonite/cellulose hybrid aerogel, corresponding to 346 eV indicating that the hybrid aerogel has been successfully prepared. Figure 5(B-D) shows the high-resolution C 1 s, Si 2p and Ca 2p spectra of MTMS-modified cellulose aerogel and MTMS-modified wollastonite/cellulose hybrid aerogel. For the MTMS-modified cellulose aerogel (Fig. 5B), the C–C/ C-H peak at 284.5 eV was the main signal peak, (Zhou et al. 2018) indicating that the -CH_3 originated from MTMS has been grafted to the wollastonite/cellulose hybrid aerogel surface. In the high-resolution Si 2p spectrum (Fig. 5C), the peak strength of the MTMS-modified wollastonite/cellulose hybrid aerogel decreased significantly, however, the Si–O of relative strength has been improved, which may be attributed to the presence of wollastonite on the aerogel surface. The covalent grafting of -CH_3 groups and the existence of crosslinking between wollastonite and cellulose are indirectly confirmed by the identification of Si–C covalent bonds by XPS analysis. Figure 5D showed peaks at 349.7 eV and 346.2 eV, proving the successful crosslink of wollastonite/cellulose hybrid aerogel. Therefore, XPS spectra confirmed the successful crosslink of wollastonite on cellulose and deposition MTMS on wollastonite/cellulose hybrid aerogel.

As known, cellulose matrix composites are essential to excellent stability as building energy saving materials. The stability of the MTMS-modified wollastonite/cellulose hybrid aerogel is evaluated by thermal analysis test and static soaking test, as shown in Fig. 6. The TG and DTG were conducted to heat-treated to 800 ℃ in flowing air of MTMS-modified wollastonite/cellulose hybrid aerogel (Fig. 6A) (Qiao et al. 2022). The weight loss on the first stage is caused by the evolution of the adsorbed H_2O and CO_2 in the porous structure of the sample, which can not be completely removed during the freeze-drying process. The weight loss in the second stage is attributed to the continuous thermal decomposition, due to the cellulose glycosidic bond in the aerogel was broken. It was decomposed by dehydration and carbonization,

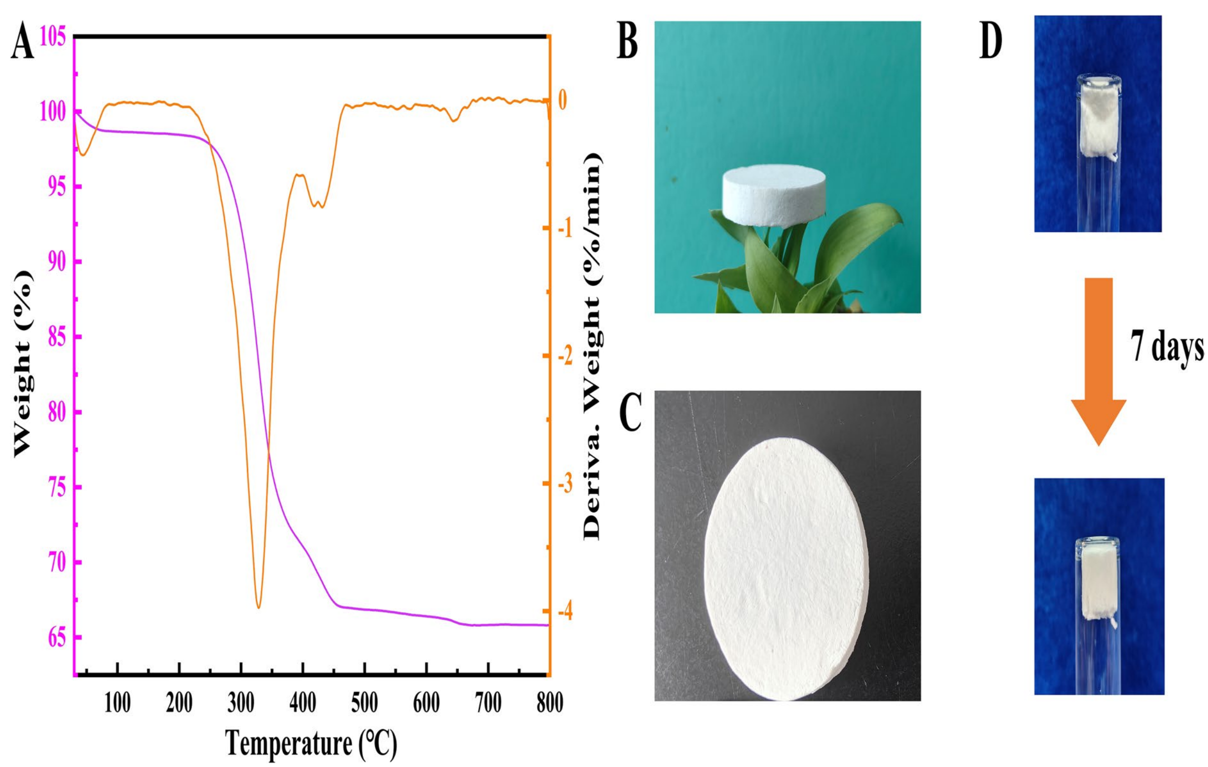

Fig. 6 **A** TG and DTG curves of MTMS-modified wollastonite/cellulose hybrid aerogel. **B** Photograph of a hybrid aerogel standing on the green plants. **C** Digital image of the MTMS-modified wollastonite/cellulose hybrid aerogel. **D** Static soaking test in water of MTMS-modified wollastonite/cellulose hybrid aerogel

the MTMS-modified wollastonite/cellulose hybrid aerogel was initially decomposed at 215 ℃. In addition, the third stage is between 400 ℃ and 470℃, when the cellulose was completely decomposed, a small amount of PPA in the aerogel for crosslinking wollastonite and cellulose begins to decompose, and the PPA is almost completely decomposed at 470℃. For the last stage (above 470 ℃), the TGA curves tend to smooth and stabilize, the remaining material being wollastonite, which was consistent with the content of wollastonite used in the experiment. The results indicate that the the addition of wollastonite may have a positive effect on the thermal stability of cellulose aerogel. Benefiting from the porous structure, the MTMS-modified wollastonite/cellulose hybrid aerogel with volume of 50.24 cm^3 exhibited lightweight property with low density of 83.59 mg/cm^3, which could easily stand on the green plants (Fig. 6B and C). Meanwhile, MTMS-modified wollastonite/cellulose hybrid aerogel showed the high porosity upward of 86.3%. The MTMS-modified wollastonite/cellulose hybrid aerogel presents a low thermal conductivity of 0.0602 W m^{-1} K^{-1}, which is slightly higher than that of the MTMS-modified wollastonite/cellulose hybrid aerogel (0.0523 W m^{-1} K^{-1}) (Table S1). The increase in thermal conductivity is mainly because of the density. Moreover, the MTMS-modified wollastonite/cellulose hybrid aerogel remains intact even after the static soaking test, which is used to evaluate the interfacial stability by soaking the sample (2 cm × 2 cm) in water at room temperature, as shown in Fig. 6D. After soaking for 7 days, the liquid in the bottle was still transparent and MTMS-modified wollastonite/cellulose hybrid aerogel did not expand, indicating that the MTMS-modified wollastonite/cellulose hybrid aerogel had good stability. Meanwhile, the successful design of the hydrophobic radiative interface was also shown by the static soaking experiment before and after the modification (Fig. S4). Therefore, MTMS-modified wollastonite/cellulose hybrid aerogel has high stability and positive effect on building materials.

High solar reflection and mid-infrared emissivity were key to realizing daytime radiative cooling. Figure 7 shows the spectral solar reflectance and infrared emissivity of MTMS-modified wollastonite/cellulose hybrid aerogel and MTMS-modified cellulose aerogel. More notably, the MTMS-modified wollastonite/cellulose hybrid aerogel has a high average reflectivity of 94.6%, owing to the porous structure and the special optical properties of wollastonite, suggesting that wollastonite particles can enhance solar reflection. The porous structure of cellulose and wollastonite had a broad distribution in the MTMS-modified wollastonite/cellulose hybrid aerogel (Fig. 2e). Such high solar reflectance minimizes the accumulation of solar heat on a surface. For MTMS-modified cellulose aerogel and MTMS-modified wollastonite/cellulose hybrid aerogel, the bonds of C–O–C and C-O provided a strong mid-infrared emission at atmospheric transparent window (Fig. S3). As expected, the mid-infrared emissive spectrum in Fig. 7A confirmed that MTMS-modified cellulose aerogel had a high mid-infrared emissivity ($\varepsilon_{LWIR} = 92.8\%$) in the range (8-13 μm). In addition, the Si–O bond in wollastonite particles cause infrared absorption at 1100–800 cm^{-1} (Fig. S3), such the emissivity ($\varepsilon_{LWIR} = 95.1\%$) of MTMS-modified wollastonite/cellulose hybrid aerogel was increased. Obviously, MTMS-modified wollastonite/cellulose hybrid aerogel was quite white and has high opacity with high reflectivity due to the synergistic effect of photon units such as micropores and wollastonite particles, indicating its excellent radiative cooling capability.

Furthermore, theoretical net cooling power of MTMS-modified wollastonite/cellulose hybrid aerogel can be calculated via the (3), (4), (5), (6), (7), (8) based on the date from emittance spectra (Note S1 in Supporting information). The calculated net cooling power (P_{net}) and achievable cooling temperatures (T_a-T_r, here T_a and T_r refer to the ambient air and the temperature of the radiative cooling device surface, respectively) of MTMS-modified wollastonite/cellulose hybrid aerogel for different nonradiative heat coefficient (q) during both day and night were demonstrated in Fig. 7B and C. In the daytime, Fig. 7B shows that the average cooling power for MTMS-modified wollastonite/cellulose hybrid aerogel was 147.4 W m^{-2} and a cooling effect of 9.8 ℃ can be achieved during the daytime when the q was 9 W m^{-2} K^{-1}. The average cooling power for MTMS-modified wollastonite/cellulose hybrid aerogel during the night was 167.4 W m^{-2}, and a cooling of 11.7 °C was possible when the q was 9 W m^{-2} K^{-1} (Fig. 7C). The calculated results show the great potential of MTMS-modified wollastonite/cellulose hybrid aerogel for PDRC applications.

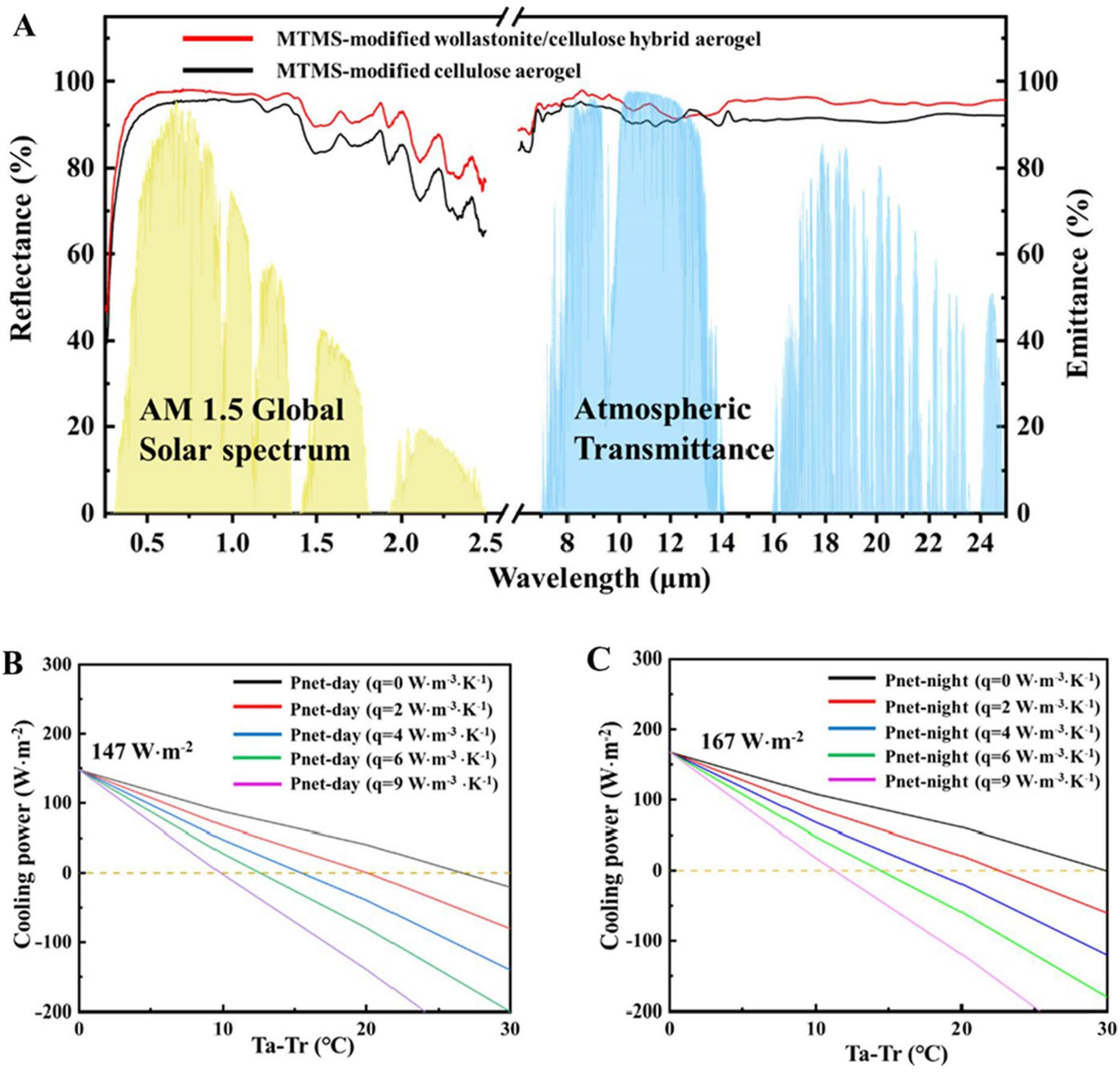

Fig. 7 **A** Spectral reflectance of the MTMS-modified wollastonite/cellulose hybrid aerogel and MTMS-modified cellulose aerogel against AM 1.5 global solar spectrum and the spectral emittance against sky windows. **B** Calculated daytime and (**C**) nighttime radiative cooling power of MTMS-modified wollastonite/cellulose hybrid aerogel

To investigate the practical radiative cooling performance of the samples more intuitively, outdoor cooling measurement were conducted on clear day in Zhenjiang, China. The sample with a thermocouple and a foam cavity was placed on a polystyrene foam box covered with a layer of Al foil to prevent the devices from being heated by reflecting solar light as shown in Fig. 8A and B (Sun et al. 2023). An ambient temperature was measured by thermocouple exposed to air. The results of the outdoor temperature test were shown in Fig. 8C, it shown a comparison of the temperature changes measured with MTMS-modified wollastonite/cellulose hybrid aerogel, MTMS-modified cellulose aerogel and ambient air over a duration of 2 h. Among all samples, benefited from excellent solar reflectance and mid-infrared emissivity, and was expected to exhibit excellent radiative cooling performance. Under the average solar intensity of 400

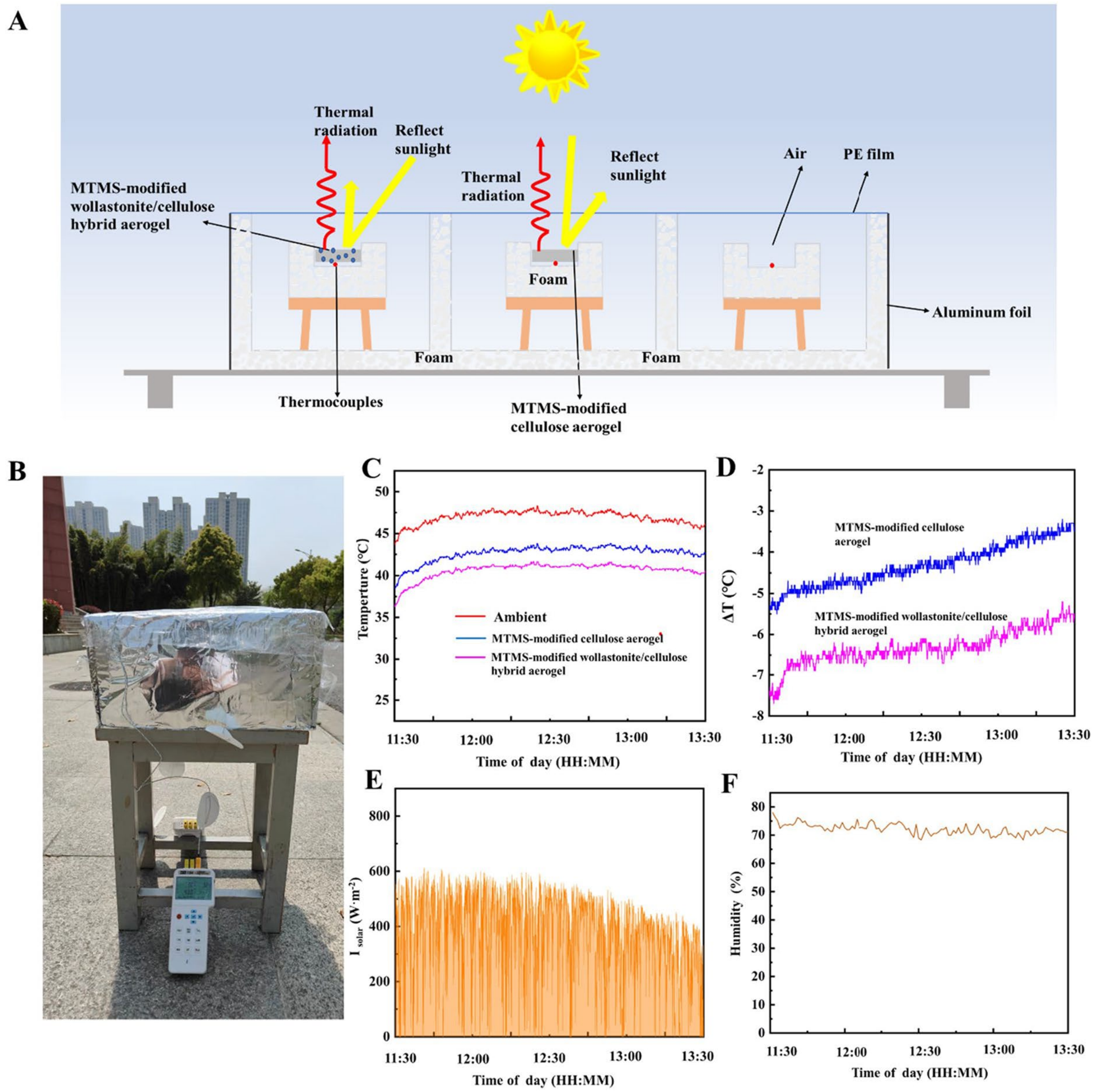

Fig. 8 **A** Schematic illustration of the measurement of radiative cooling in a thermally isolated foam box using MTMS-modified wollastonite/cellulose hybrid aerogel and MTMS-modified cellulose aerogel. **B** Photos of outdoor cooling test setup for MTMS-modified wollastonite/cellulose hybrid aerogel and MTMS-modified cellulose aerogel. **C** Temperature measurement of 2 h daytime sub-ambient cooling performance test in Zhenjiang, China. **D** Temperature difference (ΔT) of MTMS-modified wollastonite/cellulose hybrid aerogel compared to the PE covered air under daytime. **E**)The real-time I_{solar} and (**F**) the real-time relative humidity on clear day in Zhenjiang, China (119.50°E, 32.20°N, 2023/4/17 11:30 to 13:30)

W m^{-2} (Fig. 8E) and an average relative humidity of 72% (Fig. 8F), the MTMS-modified wollastonite/cellulose hybrid aerogel had the best cooling efficiency with a temperature drop of 6.3 ℃ during daytime and MTMS-modified cellulose aerogel had similar

Fig. 9 **A** Water contact angles of the samples. **B** Self-cleaning test of wollastonite/cellulose hybrid aerogel (**a**) and MTMS-modified wollastonite/cellulose hybrid aerogel (**b**). **C** Schematic of rain washes away the dust from MTMS-modified wollastonite/cellulose hybrid aerogel. **D** Schematic representation of the self-cleaning properties and PDRC performance ▶

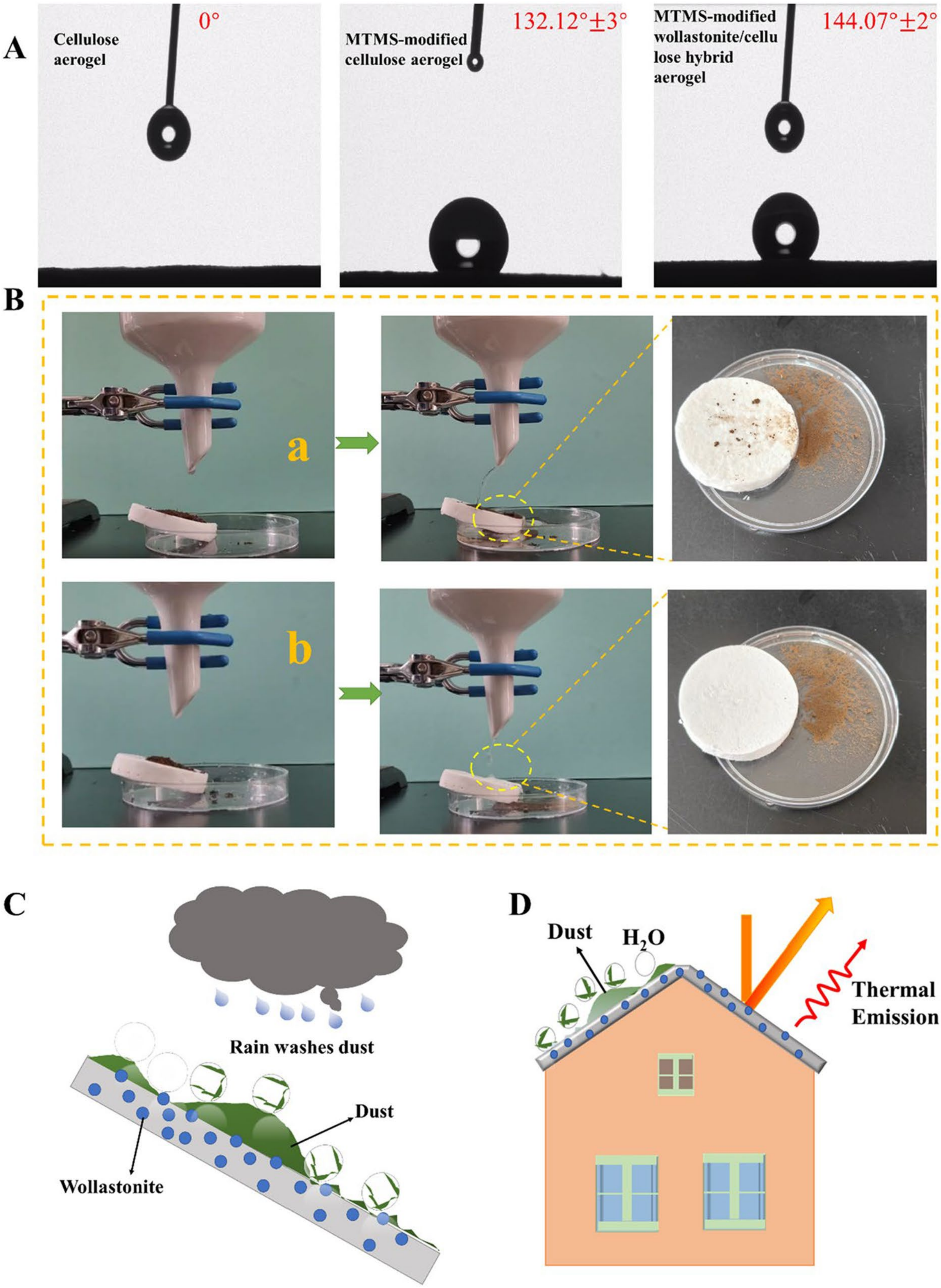
A
Cellulose aerogel
0°
MTMS-modified cellulose aerogel
132.12°±3°
MTMS-modified wollastonite/cellulose hybrid aerogel
144.07°±2°
B
a
b
C
Rain washes dust
Dust
Wollastonite
D
Dust
H2O
Thermal Emission

performance with 4.3 ℃ temperature drop (Fig. 8D). Wollastonite was introduced because it increased the material's cooling characteristics, which led to better cooling. Thus, these experiments confirmed that the obtained MTMS-modified wollastonite/cellulose hybrid aerogel could be as a high-performance radiative cooling material for applications in building energy saving.

For practical application, radiative cooling materials were expected to be used stability to apply buildings energy saving and durable enough to bear rain when exposed to open air. Benefiting from the high surface roughness, MTMS-modified wollastonite/cellulose hybrid aerogel exhibits high hydrophobicity (Tian et al. 2021). As shown in Fig. 9A, the water contact angle (WCA) of Cellulose aerogel was = 0°, indicating cellulose aerogel had excellent hydrophilic properties. However, the WCA of MTMS-modified cellulose hybrid aerogel was ≈ 132.12° ± 3°. For the MTMS-modified wollastonite/cellulose hybrid aerogel, the WCA sharply rose to 144.07° ± 2°, attributable to the elevated surface roughness generated by the wollastonite and the low surface energy groups of Si-CH_3 functional groups. As an outdoor building material, the daytime radiative cooling material must have an excellent self-cleaning ability to prevent dirt accumulation that may decrease the cooling performance. Therefore, soil particles were used as simulated contaminant to test the self-cleaning ability of MTMS-modified wollastonite/cellulose hybrid aerogel. The surface of wollastonite/cellulose hybrid aerogel was adhered by a small number of contaminants

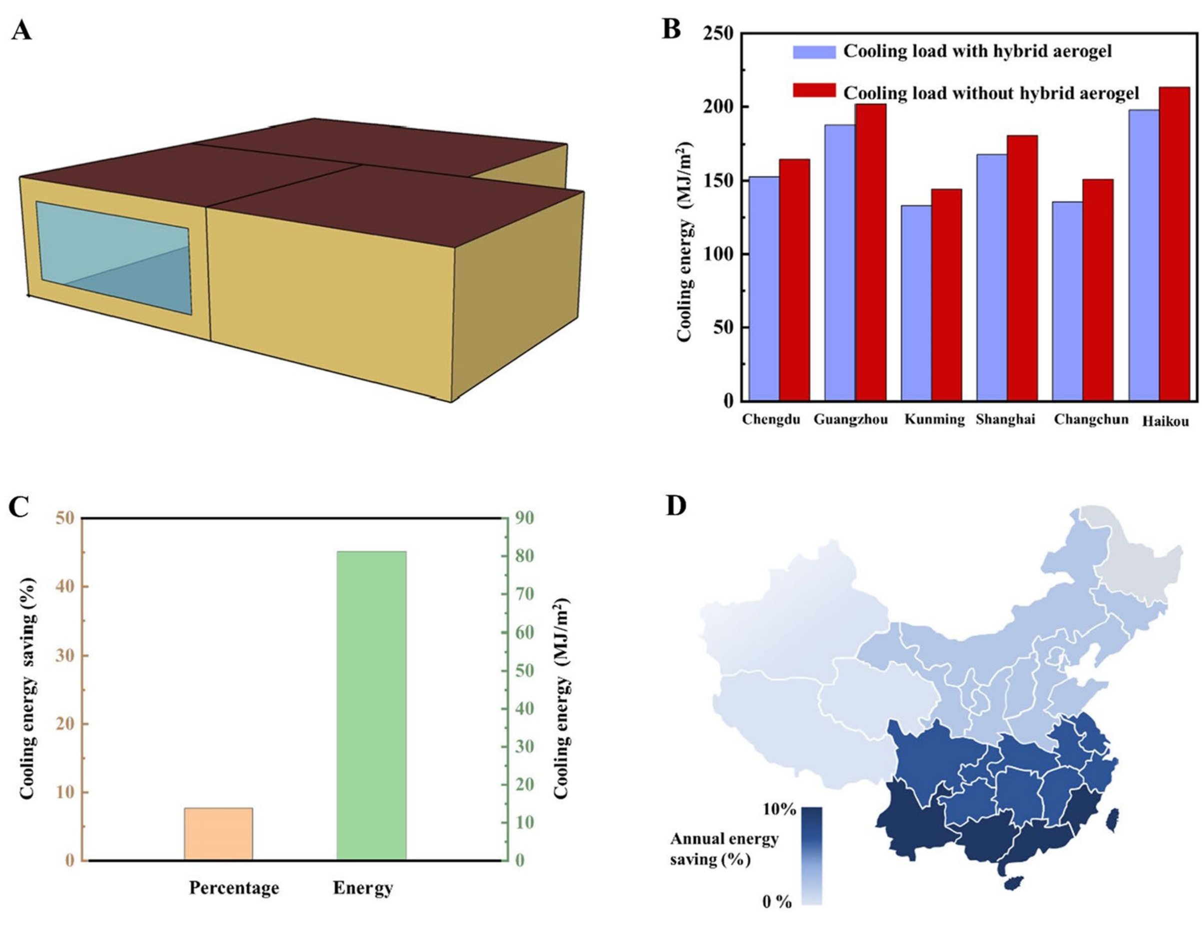

Fig. 10 **A** Structural diagram of the house used for EnergyPlus simulation. **B** Cooling energy for buildings with and without hybrid aerogel in each city. **C** The average annual cooling energy saving among all 6 cities. (**D**) The annual energy saving of buildings extend to all regions of China

and showed slight collapse (Fig. 9B(a), Video S1), while contaminants on the MTMS-modified wollastonite/cellulose hybrid aerogel surface were washed away completely leaving a clear body, as clean as the original (Fig. 9B(b), Video S2). The solar spectra of MTMS-modified wollastonite/cellulose hybrid aerogel before and after the test is shown in Fig. S5. The spectra of the MTMS-modified wollastonite/cellulose hybrid aerogel was almost identical after test, illustrating its long-term reliability. Based on this, a preliminary conclusion can be draw that the relatively rough structure formed by wollastonite on the cellulose aerogel and the chemical deposition of MTMS, rolling water droplets accumulate on the water/air interface could easy pick up the pollutants on the surface and thus realize self-cleaning as illustrated in Fig. 9C. MTMS-modified wollastonite/cellulose hybrid aerogel has excellent cooling effect and self-cleaning was demanded for buildings (Fig. 9D).

To methodically assess the potential of the hybrid aerogel for enhancing building energy efficiency, the year-round energy savings achieved by applying the hybrid aerogel to building envelope surfaces was calculated using EnergyPlus (version 23.1.0) (Fig. 10A and S6). Details of the envelope composition physical properties, and optical properties of the house are shown in the Table S2 and S3. To demonstrate the energy-saving effect of the hybrid aerogel more directly, hybrid aerogel was added to the origin building structure (including roofs), where the indoor temperature was 25 ℃, and the date of the external conditions and baseline building materials were acquired from EnergyPlus. The cooling and heating load of the building were then compared prior to and post the integration of the hybrid aerogel (Fig. 10B and S7). In this scenario, simulations were performed for typical cities in different temperature zones in China. The result show that Haikou have highest cooling energy saving potential due to their hot and dry climates. In detail, the hybrid features 8% energy saving of building baseline, correspondingly saving the cooling energy of 81.25 MJ/m^2 per year (Fig. 10C). To accurately predict the potential impact in China, the cooling energy saving of building baselines was calculated all over China (Fig. 10D), which can be affected by the regional environment (e.g. solar intensity, humidity, and latitude). These results provide valuable recommendations for the efficient implementation of hybrid aerogel in China.

Conclusions

In summary, this work demonstrated that a hybrid aerogel with self-cleaningand stable radiative perfprmance was successfully prepared by vacuum freeze-drying and chemical vapor deposition for application in building radiative cooling. The MTMS-modified wollastonite/cellulose hybrid aerogel was obtain by physiacal entanglemeng and PPA crosslinking to from porous network structure due to the strong hydrogen bonding of wollastonite and cellulose, showing excellent stability performance. Along with the strong emissivity (95.1%), MTMS-modified wollastonite/cellulose hybrid aerogel had porous structure and stable interface, resulting in a high solar reflectance (94.6%) that can effectively inhibit the heat gain from hotter surroundings. The MTMS-modified wollastonite/cellulose hybrid aerogel delivers a temperature drop of up to 6.3 ℃ under direct sunlight (solar intensity 400 W m^{-2}) in early April in Zhenjiang. Importantly, this self-cleaning property provided by high WCA (144° ± 2°) could not only keep the hybrid aerogel free from water and dust contaminants but also allowed this hybrid to maintain a good radiative cooling effect. In addition, this hybrid aerogel remained stable to static soaking for 7 days, even if the MTMS-modified wollastonite/cellulose hybrid aerogel in continuous rain environment, could maintain well stability. Meanwhile, the model results show a 8% saving of cooling energy when the hybrid aerogel is used in buildings. It was prepared in simple process and inexpensive raw materials to reduce the energy consumption of buildings, which can provide a promising direction for energy saving and sustainable radiative cooling materials.

Acknowledgements This work is supported by China Postdoctoral Science Foundation (2021T140578), Natural Science Foundation of Hebei Province (E2021108005) and 333 Talent Project Foundation of Hebei Province (A202101097).

Authors' contributions CD: Conceptualization, Methodology, Visualization, Writing-original draft, Data curation. BZ, ZW and XY: Investigation, formal analysis, validation. FQ: Supervision. DY: Supervision, writing-review and editing.

Funding Postdoctoral Science Foundation and Natural Science Foundation of Hebei Province.

Data availability All relevant data are authentic and available from the corresponding author upon request.

Declarations

Ethics approval This paper does not involve any human or animal experiments. Not applicable.

Consent for publication Not applicable.

Conflicts of interest The authors have no relevant financial or non-financial interests to disclose, and manuscript is approved by all authors for publication. I would like to declare on behalf of my co-authors that the work described was original research that has not been submitted previously.

References

Cai C, Chen F, Wei Z, Ding C, Chen Y, Wang Y, Fu Y (2023) Large scalable, anti-ultraviolet, strong cellulose film with well-defined dual-pores for longtime daytime radiative cooling. Chem Eng J 476:146668. https://doi.org/10.1016/j.cej.2023.146668

Cai C, Sun Y, Chen Y, Wei Z, Wang Y, Chen F, Cai W, Ji J, Ji Y, Fu Y (2023b) Large scalable, ultrathin and self-cleaning cellulose aerogel film for daytime radiative cooling. J Bioresourc Bioprod 8:421–429. https://doi.org/10.1016/j.jobab.2023.06.004

Chai J, Fan J (2022) Advanced thermal regulating materials and systems for energy saving and thermal comfort in buildings. Mater Today Energy 24:100925. https://doi.org/10.1016/j.mtener.2021.100925

Chen M, Li W, Tao S, Fang Z, Lu C, Xu Z (2020) A Pragmatic and High-Performance Radiative Cooling Coating with Near-Ideal Selective Emissive Spectrum for Passive Cooling. Coatings 10:144. https://doi.org/10.3390/coatings10020144

Cheng Y, Zhang S, Huan C, Oladokun MO, Lin Z (2019) Optimization on fresh outdoor air ratio of air conditioning system with stratum ventilation for both targeted indoor air quality and maximal energy saving. Build Environ 147:11–22. https://doi.org/10.1016/j.buildenv.2018.10.009

He M, Zhao B, Yue X, Chen Y, Qiu F, Zhang T (2023) Infrared radiative modulating textiles for personal thermal management: principle, design and application. Nano Energy 116:108821. https://doi.org/10.1016/j.nanoen.2023.108821

Jing W, Zhang S, Zhang W, Chen Z, Zhang C, Wu D, Gao Y, Zhu H (2021) Scalable and Flexible Electrospun Film for Daytime Subambient Radiative Cooling. ACS Appl Mater Interfaces 13:29558–29566. https://doi.org/10.1021/acsami.1c05364

Kangal MO, Bulut G, Guven O (2020) Physicochemical Characterization of Natural Wollastonite and Calcite. Minerals 10. https://doi.org/10.3390/min10030228

Li Z, Zhong L, Zhang T, Qiu F, Yue X, Yang D (2019) Sustainable, Flexible, and Superhydrophobic Functionalized Cellulose Aerogel for Selective and Versatile Oil/Water Separation. ACS Sustain Chem Eng 7:9984–9994. https://doi.org/10.1021/acssuschemeng.9b01122

Li Z, Gou M, Yue X, Tian Q, Yang D, Qiu F, Zhang T (2021) Facile fabrication of bifunctional ZIF-L/cellulose composite membrane for efficient removal of tellurium and antibacterial effects. J Hazard Mater 416:125888. https://doi.org/10.1016/j.jhazmat.2021.125888

Li T, Sun H, Yang M, Zhang C, Lv S, Li B, Chen L, Sun D (2023) All-Ceramic, compressible and scalable nanofibrous aerogels for subambient daytime radiative cooling. Chem Eng J 452:139518. https://doi.org/10.1016/j.cej.2022.139518

Lin K, Chao L, Lee HH, Xin R, Liu S, Ho TC, Huang B, Yu KM, Tso CY (2021) Potential building energy savings by passive strategies combining daytime radiative coolers and thermochromic smart windows. Case Stud Therm Eng 28:101517. https://doi.org/10.1016/j.csite.2021.101517

Lin K, Du Y, Chen S, Chao L, Him Lee H, Chung Ho T, Zhu Y, Zeng Y, Pan A, Yan Tso C (2022) Nanoparticle-polymer hybrid dual-layer coating with broadband solar reflection for high-performance daytime passive radiative cooling. Energ Buildings 276:112507. https://doi.org/10.1016/j.enbuild.2022.112507

Mandal J, Fu Y, Overvig AC, Jia M, Sun K, Shi NN, Zhou H, Xiao X, Yu N, Yang Y (2018) Hierarchically porous polymer coatings for highly efficient passive daytime radiative cooling. Science 362:315–319. https://doi.org/10.1126/science.aat9513

Meir MG, Rekstad JB, LØvvik OM (2002) A study of a polymer-based radiative cooling system. Sol energy 73:403–417. https://doi.org/10.1016/S0038-092X(03)00019-7

Qiao A, Huang R, Penkova A, Qi W, He Z, Su R (2022) Superhydrophobic, elastic and anisotropic cellulose nanofiber aerogels for highly effective oil/water separation. Sep Purif Technol 295:121266. https://doi.org/10.1016/j.seppur.2022.121266

Rephaeli E, Raman A, Fan S (2013) Ultrabroadband Photonic Structures To Achieve High-Performance Daytime Radiative Cooling. Nano Lett 13:1457–1461. https://doi.org/10.1021/nl4004283

Shang S, Ye X, Jiang X, You Q, Zhong Y, Wu X, Cui S (2021) Preparation and characterization of cellulose/attapulgite composite aerogels with high strength and hydrophobicity. J Non-Cryst Solids 569:120922. https://doi.org/10.1016/j.jnoncrysol.2021.120922

She X, Cong L, Nie B, Leng G, Peng H, Chen Y, Zhang X, Wen T, Yang H, Luo Y (2018) Energy-efficient and -economic technologies for air conditioning with vapor compression refrigeration: A comprehensive review. Appl Energ 232:157–186. https://doi.org/10.1016/j.apenergy.2018.09.067

Song J, Qin J, Qu J, Song Z, Zhang W, Xue X, Shi Y, Zhang T, Ji W, Zhang R, Zhang H, Zhang Z, Wu X (2014) The effects of particle size distribution on the optical properties of titanium dioxide rutile pigments and their applications in cool non-white coatings. Sol Energ Mat Sol C 130:42–50. https://doi.org/10.1016/j.solmat.2014.06.035
Soulios V, Loonen RCGM, Metavitsiadis V, Hensen JLM (2018) Computational performance analysis of overheating mitigation measures in parked vehicles. Appl Energ 231:635–644. https://doi.org/10.1016/j.apenergy.2018.09.149
Sun Z, Bai Z, Shen H, Zheng S, Frost RL (2013) Electrical property and characterization of nano-SnO_2/wollastonite composite materials. Mater Res Bull 48:1013–1019. https://doi.org/10.1016/j.materresbull.2012.11.087
Sun Y, He H, Huang X, Guo Z (2023) Superhydrophobic SiO_2–Glass Bubbles Composite Coating for Stable and Highly Efficient Daytime Radiative Cooling. ACS Appl Mater Interfaces 15:4799–4813. https://doi.org/10.1021/acsami.2c18774
Tang W, Jian Y, Shao M, Cheng Y, Liu J, Liu Y, Hess DW, Wan H, Xie L (2023) A novel two-step strategy to construct multifunctional superhydrophobic wood by liquid-vapor phase deposition of methyltrimethoxysilane for improving moisture resistance, anti-corrosion and mechanical strength. Colloid Surface A 666:131314. https://doi.org/10.1016/j.colsurfa.2023.131314
Tian Q, Qiu F, Yue X, Li Z, Zhao B, Zhang T (2021) Surface structure regulation of wastewater flocculated sludge for hierarchical superhydrophobic ceramic coating. J Environ Chem Eng 9:106851. https://doi.org/10.1016/j.jece.2021.106851
Wang J, Liu S (2019) Remodeling of raw cotton fiber into flexible, squeezing-resistant macroporous cellulose aerogel with high oil retention capability for oil/water separation. Sep Purif Technol 221:303–310. https://doi.org/10.1016/j.seppur.2019.03.097
Xiang B, Zhang R, Luo Y, Zhang S, Xu L, Min H, Tang S, Meng X (2021) 3D porous polymer film with designed pore architecture and auto-deposited SiO_2 for highly efficient passive radiative cooling. Nano Energy 81:105600. https://doi.org/10.1016/j.nanoen.2020.105600
Xue S, Lv X, Liu N, Zhang Q, Lei H, Cao R, Qiu F (2023) Electrocatalytic Hydrogen Evolution of Bent Bis(dipyrrin) Ni(II) Complexes. Inorg Chem 62:1679–1685. https://doi.org/10.1021/acs.inorgchem.2c04097
Yue X, Wu H, Zhang T, Yang D, Qiu F (2022) Superhydrophobic waste paper-based aerogel as a thermal insulating cooler for building. Energy 245:123287. https://doi.org/10.1016/j.energy.2022.123287
Zhang S, Jing W, Chen Z, Zhang C, Wu D, Gao Y, Zhu H (2022) Full daytime sub-ambient radiative cooling film with high efficiency and low cost. Renew Energ 194:850–857. https://doi.org/10.1016/j.renene.2022.05.151
Zhao B, Lu K, Hu M, Liu J, Wu L, Xu C, Xuan Q, Pei G (2022a) Radiative cooling of solar cells with micro-grating photonic cooler. Renew Energ 191:662–668. https://doi.org/10.1016/j.renene.2022.04.063
Zhao B, Yue X, Tian Q, Qiu F, Zhang T (2022b) Controllable fabrication of ZnO nanorods@cellulose membrane with self-cleaning and passive radiative cooling properties for building energy-saving applications. Cellulose 29:1981–1992. https://doi.org/10.1007/s10570-021-04408-2
Zheng Y, Wang C, Zhou S, Luo C (2021) The self-gelation properties of calcined wollastonite powder. Constr Build Mater 290:123061. https://doi.org/10.1016/j.conbuildmat.2021.123061
Zhou S, You T, Zhang X, Xu F (2018) Superhydrophobic Cellulose Nanofiber-Assembled Aerogels for Highly Efficient Water-in-Oil Emulsions Separation. ACS Appl Nano Mater 1:2095–2103. https://doi.org/10.1021/acsanm.8b00079
Zhu Y, Li H, Huang W, Lai X, Zeng X (2023) Facile fabrication of superhydrophobic wood aerogel by vapor deposition method for oil-water separation. Surf Interfaces 37:102746. https://doi.org/10.1016/j.surfin.2023.102746